Structure, Vol. 12, 1955–1965, November, 2004, ©2004 Elsevier Ltd. All rights reserved. DOI 10.1016/j.str.2004.09.003

The Crystal Structure of RhoA in Complex with the DH/PH Fragment of PDZRhoGEF, an Activator of the Ca^{2+} Sensitization Pathway in Smooth Muscle

Urszula Derewenda,[1] Arkadiusz Oleksy,[2] Andra S. Stevenson,[1] Justyna Korczynska,[1] Zbigniew Dauter,[3] Andrew P. Somlyo,[1,4] Jacek Otlewski,[2] Avril V. Somlyo,[1,*] and Zygmunt S. Derewenda[1,*]

[1]Department of Molecular Physiology and Biological Physics
University of Virginia
Charlottesville, Virginia 22908

[2]Laboratory of Protein Engineering
Institute of Biochemistry and Molecular Biology
University of Wrocław
Tamka 2
50-137 Wrocław
Poland

[3]Synchrotron Radiation Research Section
Macromolecular Crystallography Laboratory
NCI, Brookhaven National Laboratory
Upton, New York 11973

Summary

Calcium sensitization in smooth muscle is mediated by the RhoA GTPase, activated by hitherto unspecified nucleotide exchange factors (GEFs) acting downstream of $G\alpha q/G\alpha_{12/13}$ trimeric G proteins. Here, we show that at least one potential GEF, the PDZRhoGEF, is present in smooth muscle, and its isolated DH/PH fragment induces calcium sensitization in the absence of agonist-mediated signaling. In vitro, the fragment shows high selectivity for the RhoA GTPase. Full-length fragment is required for the nucleotide exchange, as the isolated DH domain enhances it only marginally. We crystallized the DH/PH fragment of PDZRhoGEF in complex with nonprenylated human RhoA and determined the structure at 2.5 Å resolution. The refined molecular model reveals that the mutual disposition of the DH and PH domains is significantly different from other previously described complexes involving DH/PH tandems, and that the PH domain interacts with RhoA in a unique mode. The DH domain makes several specific interactions with RhoA residues not conserved among other Rho family members, suggesting the molecular basis for the observed specificity.

Introduction

Increased Ca^{2+} sensitivity (or Ca^{2+} sensitization) in smooth muscle is a result of a higher level of phosphorylation of the regulatory light chain of myosin, with concomitant increased tension at constant submaximal Ca^{2+} concentration. This phenomenon occurs in response to agonist stimulation and the resultant RhoA-mediated inhibition of the myosin light chain phosphatase (MLCP). Experiments using permeabilized muscles that retain G protein-coupled receptors established that this pathway can also be activated by GTPγS while Ca^{2+} is clamped (Kitazawa et al., 1989). Different agonists can stimulate unequal maximal Ca^{2+} sensitization (Himpens et al., 1990), acting through trimeric G proteins of the $G\alpha_q$, $G\alpha_{12}$, and $G\alpha_{13}$ families and the RhoA GTPase (Gong et al., 1996). Calcium sensitization has broad implications for health, disease, and therapy (Somlyo and Somlyo, 2003), but many of its aspects are not well understood. One of the important unresolved questions is the nature of the coupling of the trimeric G proteins and RhoA, which is most likely mediated by RhoA-specific members of the Dbl family of nucleotide exchange factors, or GEFs (Schmidt and Hall, 2002; Whitehead et al., 1997). A majority of known GEFs in this family are multidomain proteins of crucial physiological significance acting downstream of the tyrosine-kinase family of receptors, but at least one family is activated by G protein-coupled receptors via an RGSL (RGS-like) domain capable of binding the α chain of $G_{12/13}$ (Fukuhara et al., 1999, 2000; Hart et al., 1998; Kozasa et al., 1998; Suzuki et al., 2003). This unique family showing distinct homology includes PDZRhoGEF (Fukuhara et al., 1999; Rumenapp et al., 1999), also known as GTRAP48 (Jackson et al., 2001), p115RhoGEF (Kozasa et al., 1998), and LARG, or the leukemia-associated RhoGEF (Fukuhara et al., 2000). An RGSL domain was also recently discovered in another, more distantly related exchange factor, Lbc (Dutt et al., 2004). The crystal structures of the RGSL domains from PDZRhoGEF and p115 have been solved, and models of interactions with $G\alpha$ have been proposed (Chen et al., 2001; Longenecker et al., 2001), but the exact mechanism by which this interaction may activate the nucleotide exchange function of the GEF molecule is not known.

All GEFs active on the Rho family of GTPases catalyze the GDP/GTP exchange by stabilizing the nucleotide-free form of the GTPase, using a tandem of DH (Dbl-homology) and PH (pleckstrin-homology) domains, thereby allowing the more abundant in vivo GTP to replace GDP. Many aspects of the molecular mechanism by which this is accomplished have been revealed by the crystal structures of complexes of the Tiam1 DH-PH tandem with Rac1 (Worthylake et al., 2000); the ITSN (intersectin) DH-PH tandem with Cdc42 and the Dbs (DH-PH) with RhoA (Snyder et al., 2002); and Dbs (DH-PH) with Cdc42 (Rossman et al., 2002). These studies have shown that while all the residues essential for the nucleotide exchange process are found in the DH domain, the PH domain, at least in some cases, contributes substantially to the selectivity and specificity of interactions.

Given the presence of the RGSL domain in PDZRhoGEF and its homologs, and because of the high selectivity that these GEFs show for RhoA as their substrate, we considered the possibility that at least some of the family members might be involved in the Ca^{2+} sensitiza-

*Correspondence: zsd4n@virginia.edu (Z.S.D.), avs5u@virginia.edu (A.V.S.)
[4]Deceased.

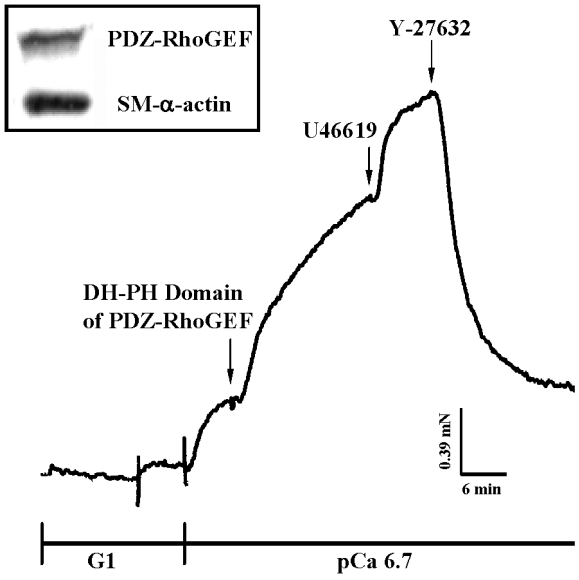

Figure 1. Representative Tension Trace Illustrating the Protocol for Eliciting the PDZRhoGEF-Induced Ca^{2+}-Sensitization and Its Inhibition by the Rho-Kinase Inhibitor Y-27632 in β-Escin Permeabilized Pulmonary Artery Smooth Muscle.

Following permeabilization, submaximal tension was developed in pCa 6.7 solution before addition of 50 μM solution of the recombinant DH-PH fragment of PDZRhoGEF. At the plateau of Ca^{2+} sensitization induced by the domain, the addition of U46619, a thromboxane A_2 analog, caused an additional increase in contraction. Contraction could be rapidly inhibited by 10 μM Y-27632 inhibitor. These data are representative of three experiments. Inset: Western blot showing evidence of expression of PDZRhoGEF in rabbit pulmonary artery smooth muscle.

tion pathway. Indeed, we find that the PDZRhoGEF protein is present in smooth muscle. In this paper, we present in vitro and in vivo functional studies of the recombinant DH/PH fragment of PDZRhoGEF, as well as the 2.5 Å resolution crystal structure of its complex with nonprenylated RhoA. The structure reveals the molecular details that constitute the basis for the observed RhoA selectivity.

Results and Discussion

PDZRhoGEF Is Present in Smooth Muscle Tissue

The key role of RhoA in the Ca^{2+} sensitization pathway downstream of G protein-coupled receptors implies the presence of a signaling route involving RhoA-specific GEFs interacting with trimeric G proteins. Among few potential candidates, PDZ-RhoGEF has been shown by others to interact with heterotrimeric G proteins of the $G\alpha_{12}$ family. Here, we have identified PDZRhoGEF in the whole homogenate of rabbit pulmonary artery smooth muscle tissue by Western blot analysis, as described in Experimental Procedures (Figure 1, inset).

The DH/PH Fragment of PDZRhoGEF Is Sufficient for Eliciting Ca^{2+} Sensitization

Given the presence of PDZRhoGEF in the smooth muscle, we wondered if the isolated DH/PH fragment of PDZRhoGEF (residues 712–1081) could act as the sole activator of the Ca^{2+} sensitization pathway. The underlying hypothesis was that in the absence of other domains that might exert downregulation, the DH/PH fragment should be constitutively active. To test this, a recombinant DH/PH fragment of PDZ-RhoGEF was purified and used in isometric tension measurements using permeabilized rabbit pulmonary artery strips, as described in Experimental Procedures. The presence of the exogenous DH/PH fragment reproducibly resulted in a significant increase in force at constant Ca^{2+} concentration, pCa 6.7 (16.6 ± 3.3% of the maximal contraction at pCa 4.5) (Figure 1). Addition of the filtrate of the DH-PH fragment was without effect on force. The addition of U46619, an activator of $G\alpha_{12/13}$-coupled thromboxane A2 receptors, caused a further increase in contraction, illustrating that agonist-G protein-coupled receptor activation of the Ca^{2+} sensitization pathway is intact in this permeabilized muscle preparation. The increase in force was abolished by the Y-27632 Rho-kinase inhibitor at 10 μM concentration, suggesting—as expected—a role for Rho-kinase in the activation of Ca^{2+} sensitization mediated by the DH/PH fragment.

The DH/PH Fragment Is Highly Selective In Vitro for RhoA

Having established the physiological effect of the DH/PH fragment, we asked if the presence of the DH/PH fragment leads to selective activation of the RhoA GTPase. Although a larger fragment encompassing the DH/PH tandem and the C-terminal domain of PDZRhoGEF (residues 637–1522) has been shown to selectively catalyze the nucleotide exchange for RhoA (Rumenapp et al., 1999) no rigorous in vitro functional studies were reported to date for the isolated DH/PH fragment or the DH domain. Using a fluorimetric assay described in Experimental Procedures, we measured intrinsic nucleotide exchange rates for RhoA, Cdc42, and Rac1, and then assessed the acceleration of the reaction in the presence of either the isolated DH domain, or of the intact DH/PH fragment (Figure 2, Table 1). The rate of exchange increases more than two orders of magnitude for RhoA in the presence of the DH/PH fragment, and only 7-fold for Cdc42. There is no detectable effect on Rac1. In contrast, the Dbs DH/PH fragment was reported to catalyze ~50-fold enhancements of the reaction rates for Cdc42 and RhoA, while intersectin is strictly selective for Cdc42, with a similar catalytic effect (Cheng et al., 2002; Rossman et al., 2002; Snyder et al., 2002). Neither protein catalyzes nucleotide exchange for Rac.

The isolated DH domain is capable of only a 5-fold enhancement of the nucleotide exchange for RhoA, indicating that the PH domain plays a critical role for both the catalytic function of the GEF and for its selectivity. In fact, this pattern of PH-assisted catalysis is virtually identical to that observed for Dbs and Trio (Liu et al., 1998; Rossman and Campbell, 2000), but unlike intersectin, whose DH domain does not require the PH domain for catalysis (Pruitt et al., 2003).

The Crystal Structure of the DH/PH-RhoA Complex: An Overview

In order to rationalize the observed functional properties of the DH/PH fragment, we solved its crystal structure in

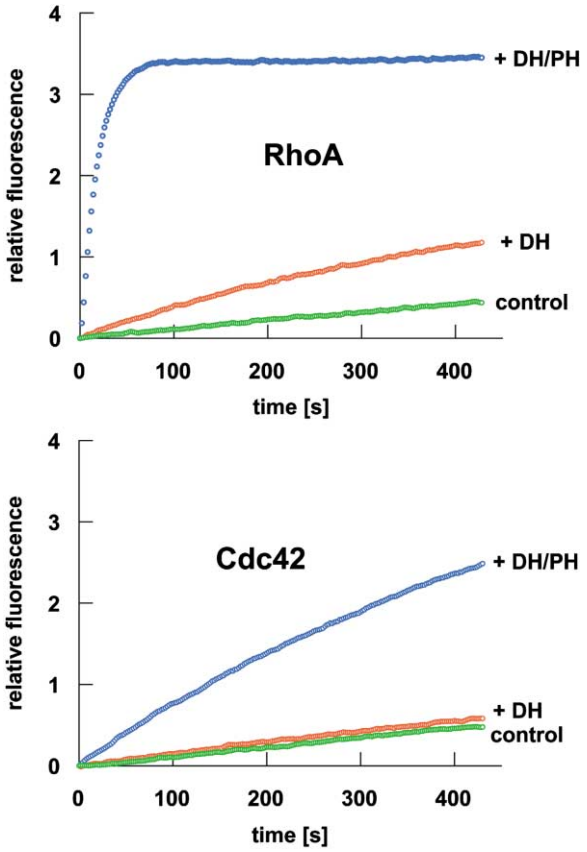

Figure 2. Guanine Nucleotide Exchange Activity of RhoA (1–193) and Cdc42 (1–191) Stimulated by DH Domain and DH/PH Tandem of PDZ-RhoGEF (In Vitro)

The rate of exchange reaction was monitored by increase in the mant-GTP fluorescence intensity as a result of its incorporation to the GTPase, as described in Experimental Procedures. Intrinsic exchange activities of RhoA and Cdc42 are shown as a control experiment (dark green circles). The rate of nucleotide exchange stimulated by DH domain (red circles) and DH/PH tandem (blue circles) was estimated by linear regression analysis of approximately the first 50 s after DH stimulation and 12 s after DH/PH stimulation.

complex with the nonprenylated, C-terminally truncated RhoA (residues 1–181). The crystals contain two copies of the complex within the asymmetric unit. The two are very similar and superpose with the rms difference of 0.93 Å for all 533 Cα atoms. The electron density is well-defined for most residues in the RhoA molecules and in the DH domains. No unaccounted density is found in the nucleotide binding pocket, consistent with the notion that RhoA is nucleotide-free. In contrast, the PH domains are less well defined and the mean isotropic displacement (B) parameters of the DH domains and RhoA molecules are lower than those of the PH domains (~53 Å^2 for the DH and ~63 Å^2 for RhoA versus ~87 Å^2 for the PH domains). Thus, each of the PH domains appears to have a significant degree of freedom within the crystal lattice in spite of interacting with both its partner DH domain and the RhoA GTPase. The two complexes differ slightly in the dispositions of the DH and PH domains relative to the RhoA GTPase. Specifically, least-squares superposition of the complexes on RhoA reveals that that the DH domains are minimally rotated with respect to each other by ~2.5° around an axis approximately perpendicular to the interface. The two PH domains are rotated by ~4°. These minor conformational variations do not affect the detailed architecture of the interfaces discussed in this paper. Furthermore, the similarity of the two complexes constrained in the crystal lattice by two different sets of crystal contacts strongly suggests that the observed conformations are representative of that in solution. For the purposes of subsequent analysis, we treat the two complexes as identical.

As in the other previously reported crystal structures of similar complexes, the interaction with the DH/PH fragment alters the local structure of the two functionally important switch regions in RhoA, thus stabilizing the nucleotide free form (Figure 3A). The structure of RhoA in the complex described here is virtually identical to that described in the Dbs complex (Snyder et al., 2002).

Both the DH and PH domains show extensive similarities—as expected—to other members of their respective families. The DH domain (Figure 3A) is an elongated helical bundle, as originally described for SOS and betaPIX (Aghazadeh et al., 1998; Soisson et al., 1998), and assumes a "chaise lounge" shape with all the long helices (α1a, α2b, α3a, α5b, and α6) packed into the long "seat" and the short helices (α3c, α4a, α4b, and α5a) in the "seatback." Here, we follow the standard nomenclature proposed for these domains by Rossman et al. (2002) that uses the six major helices as the reference points to describe the structure. Among the structurally characterized DH domains, the PDZRhoGEF DH domain is most similar to that of intersectin (PDB entry 1KI1), with which it also shares the highest level of sequence identity (~31%), although not the GTPase preference (Figure 3B). A total of 208 equivalent Cα atoms (out of 226 possible) superpose with an rms difference

Table 1. Nucleotide Exchange Rates of Intrinsic, DH-Stimulated, and DH/PH-Stimulated Reactions on RhoA, Cdc42, and Rac1 GTPases

	Control[a] (RF[b] $s^{-1} \times 10^{-3}$)	DH-stimulated (RF[b] $s^{-1} \times 10^{-3}$)	FS[c]	DH/PH-stimulated (RF[b] $s^{-1} \times 10^{-3}$)	FS[c]
RhoA (1–193)	1	4.4	4.4 ×	136	136 ×
RhoA (1–181)	0.6	3	5 ×	125	208 ×
Cdc42 (1–191)	1.1	1.3	1.2 ×	7.8	7.1 ×
Rac1 (1–192)	0.7	0.7	1 ×	0.7	1 ×

[a] Control experiment indicates intrinsic (nonstimulated) exchange activity of a given GTPase.
[b] RF–relative fluorescence signal (λ_{ex} = 356 nm, λ_{em} = 445 nm)
[c] FS–fold stimulation value; reflects the ratio of the initial exchange rate of DH- or DH/PH- stimulated reaction to the intrinsic rate of exchange for given GTPase.

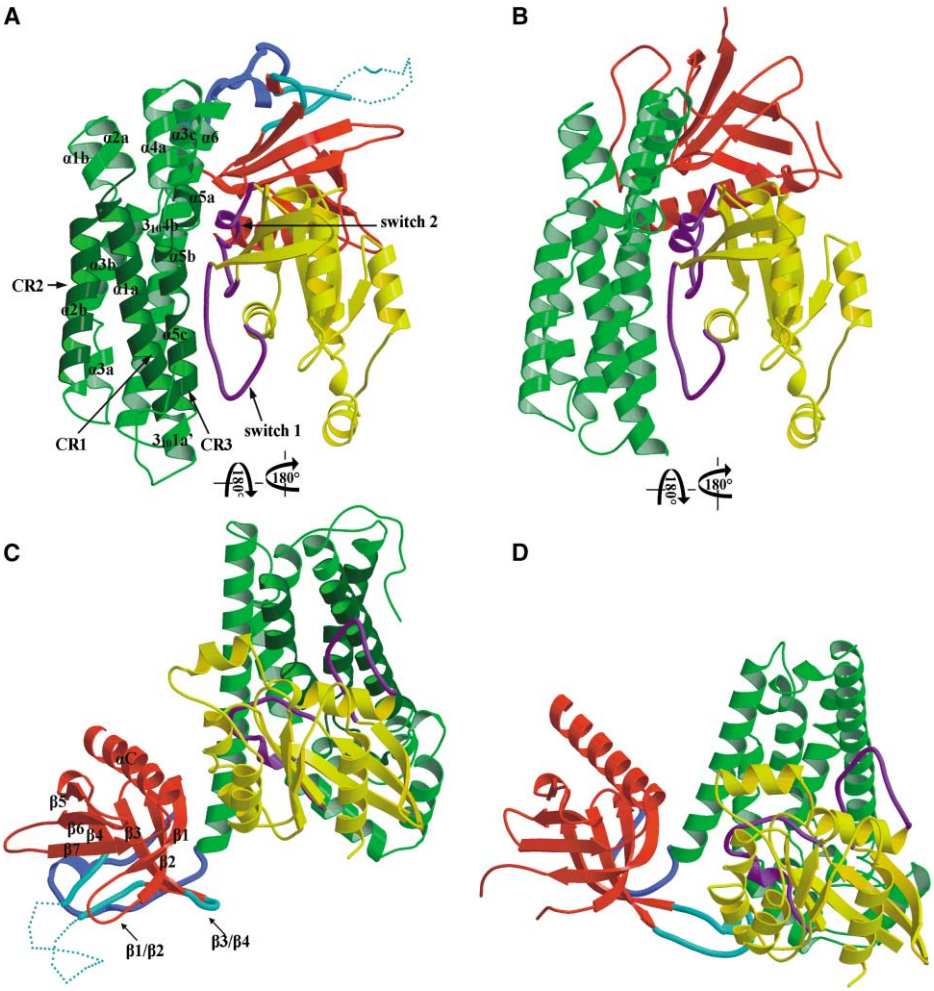

Figure 3. The Crystal Structure of the RhoA in Complex with the DH/PH Fragment of PDZRhoGEF and Its Comparison to Complexes with Intersectin and Dbs

(A) The general features of the DH-domain (green)–RhoA (yellow) interface, with the PH domain (red) at the rear; the two switch regions of RhoA are shown in purple and labeled; the CR regions of the DH domain are dark green and labeled.

(B) A comparable view of the intersectin's DH/PH fragment in complex with Cdc42–1KI1.PDB.

(C) A rotated view of the complex shown in A, with the PH domain (red) into the foreground; the unique β4 bulge is shown in turquoise with the dashed line indicating poorly defined fragment, and dark blue indicates the linker region between the DH and PH domains; the DH domain in the background is green.

(D) A comparable view of the Dbs DH/PH fragment in complex with RhoA–1LB1.PDB.

of ~1.6–1.8 Å. In contrast, both TIAM1 and Dbs GEFs, acting on Rac and RhoA/Cdc42, respectively, deviate significantly with pairwise rms differences above 3 Å and sequence identity levels of ~21% for TIAM1 and ~24% for Dbs. The closest fit between the DH domains of intersectin and PDZRhoGEF is in the CR1 and CR3 regions. The CR2 region, which is distal to the GTPase binding site, fits marginally less well. Thus, the best fit between the two structures is in the long seat part, while the seatback is slightly rearranged.

The PH domain, like other domains in this family, forms an antiparallel β sandwich capped by a short C-terminal α-helix (Rebecchi and Scarlata, 1998). The sandwich is made up of two, nearly orthogonal, β sheets with four β strands (β1–β4) in the first, N-terminal β sheet and three strands (β5–β7) in the second β sheet (Figure 3C). The hydrophobic core contains residues originating from all β strands and the C-terminal helix, among them the completely buried Leu993, Leu995, Leu1026, Leu1059, and Ile1045. The PDZRhoGEF PH domain is similar in its architecture to the PH module of Dbs, with which it shares ~23% amino acid sequence identity (Figure 3D). The superposition of the two domains results in a root-mean-square difference of ~1.6 Å on 97 Cα atoms, with the β strands and the C-terminal helix showing the highest similarity. A distinctive feature of the PH domain of PDZRhoGEF is an 18-residue insertion in the β4 strand, between Leu1005 and Pro1024. This insertion is similar to a special wide (SW) category of β-bulges (Chan et al., 1993), except that Pro1024—which is in the αR conformation—is an unusual residue at this position. We were unable to find another insertion of this type among any other PH domains. The resulting bulge in the tertiary fold protrudes into the canonical phosphoinositide bind-

ing site and shows high conformational flexibility as judged by the relatively poor quality of the electron density, particularly in the solvent exposed fragment. The other major differences between the PH domains of PDZRhoGEF and Dbs are at the splayed end due to very different conformations of the β1/β2 loop, which is ~10 amino acids longer in Dbs, and the β3/β4 loop, also significantly longer in Dbs.

It has been noted, that many PH domains are strongly polarized (Lemmon et al., 2002; Macias et al., 1994). Most canonical PH domains have a positive potential at the "bottom" splayed end of the structure, between the β1/β2 and β3/β4 loops, where they bind phosphoinositides. In Dbs, the region of the β1/β2 loop contains five Lys and Arg residues and four more on the β3 and β4 strands. In the case of the PDZRhoGEF PH domain, the β1/β2 loop has only three positively charged residues counterbalanced by two aspartates. Three more positive charges are found on the β4 strand, but overall the positive potential is much weaker, suggesting that phosphoinositol binding may not be a primary function of this protein, although no experimental data to confirm this notion have been reported. In addition, as already pointed out, the putative phosphoinositol binding pocket is partially filled with a long β-bulge originating from the β4 strand.

The DH-RhoA Interface

The interface between the DH domain and RhoA is similar to that observed in other complexes of this type involving the DH/PH fragments of TIAM1, Dbs, and intersectin (Karnoub et al., 2001; Rossman et al., 2002; Snyder et al., 2002). RhoA buries a total of 1,467 Å^2 of solvent accessible surface. The interface is formed primarily by the contacts between the residues in the conserved regions (CR) CR1 and CR3 of the DH domain and switch I of RhoA, and by the contacts between a segment just preceding and involving the CR3 region and the α6 helix of DH, and switch II of RhoA (Figure 4).

The interactions involving switch I of RhoA are generic for Rho GTPases, particularly that of Glu741^{DH} with the backbone amides of Thr37^{RhoA} and Val38^{RhoA}, as well as the side chain hydroxyl of Tyr34^{Rhoa}. These interactions stabilize the switch I region of all Rho GTPases in the known complexes in the same conformation.

The switch II interactions in the known complexes, which define the selectivity for the GTPase, are centered on a bulky residue on the surface of the GTPase (Trp58 in RhoA, Trp56 in Rac, and Phe56 in Cdc42) nested in a molecular cradle created by a set of residues in the α5a helix of the DH domain. In the present structure this paradigm is preserved, and the "cradle" is formed by Leu869^{DH}, Asp873^{DH}, and Ile876^{DH}. Particularly interesting is the side chain of Asp873^{DH}, which is locked into its conformation by an H-bond accepted by Oδ2 from the backbone amide of Gln870^{DH} (otherwise unpaired) and an apparent C-H…O bond from the Cζ2 atom of the indole ring of Trp58^{RhoA}. The Cζ2(Trp58)-Oδ1(Asp73) distances in the two molecules are 3.2 Å and 3.3 Å respectively with suitable geometry. The C-H….O bonds are increasingly recognized as a general structural feature in proteins (Derewenda et al., 1995), contributing significantly to protein-ligand (Pierce et al., 2002) and protein-protein interactions (Jiang and Lai, 2002). More recently it has been noted that –CH groups within the indole ring of tryptophans are often donors of such weak, but structurally important H-bonds (Petrella and Karplus, 2004). In addition to this weak interaction with Trp58^{RhoA}, Asp873^{DH} also forms an energetically more important salt bridge with Arg5^{RhoA}. This is one of several salt bridges that flank the Trp58-centered interface, including those formed by Arg868^{DH} with both Asp45^{RhoA} and Glu54^{RhoA}, Arg872^{DH} with Asp76^{RhoA}, and Arg867^{DH} with Glu40^{RhoA}. Finally, there are a few hydrophobic interactions in this interface, with the most prominent one involving Met879^{DH} on one side and Leu69^{RhoA} and Leu72 ^{RhoA} on the other.

An additional interaction involves the switch II region of RhoA and helix α6 of the DH domain. The side chain of Arg 68^{RhoA}, a residue conserved among all Rho GTPases, makes a double salt bridge with Glu928^{DH} and Asn929^{DH}. In addition, the backbone amide of Arg68^{RhoA} donates an H-bond to the side chain of Asp921^{DH}. Glu928^{DH} corresponds to Glu1428^{DH} and Glu1239^{DH} in intersectin and TIAM1, respectively, and so the salt bridge may have a generic significance for these GEFs. In contrast, in each of the Dbs complexes, Arg68 of the GTPase interacts with the backbone carbonyl of 887^{DH} and with the side chain hydroxyl of Tyr889^{DH}.

The interaction involving switch II and the α6 helix of the DH domain may contribute to the integrity and stability of the α6 helix and therefore to the stability of the whole complex. In Dbs, the α6 helix in the DH/PH fragment appears to be stable in both of its complexes with GTPases, as inferred from the respective crystal structures. In contrast, the structure of the isolated Dbs DH/PH fragment shows that in the absence of the GTPase the α6 helix may bend away from the body of the DH domain, thus altering the relative position of the PH domain; this is seen in two out of four copies of the DH/PH molecule in the asymmetric unit (Worthylake et al., 2004). It is possible that the C-terminal part of the α6 helix requires stabilization provided by protein-protein interactions. The linker connecting the DH and PH domains, as well as the PH domain itself, makes several contacts with the C terminus of the α6 helix. To date, no structure is available for any of the isolated DH domains from the relevant DH/PH fragments, and no comparisons are possible, but it is likely that without the PH domain the conformation of the α6 helix might be altered and the interactions with the GTPase would be lost.

The Orientation of the PH Domain in the Complex

The most significant diversity between the known structures of DH/PH GEF fragments in complexes with their cognate GTPases is in the position of the PH domain relative to the DH-GTPase interface. This variation stems from the differences in the length of the C-terminal (α6) helix of the DH domain, as well as a rotation of the PH domain around the α6 helix. The shortest helix—26 residues—is seen in Dbs (Figure 5A). In other complexes, namely Tiam1, ITSN, and PDZ-RhoGEF, the α6 helix is 10 to 13 amino acids longer. In this regard, the TIAM1 α6 helix is between that of Dbs on the one hand,

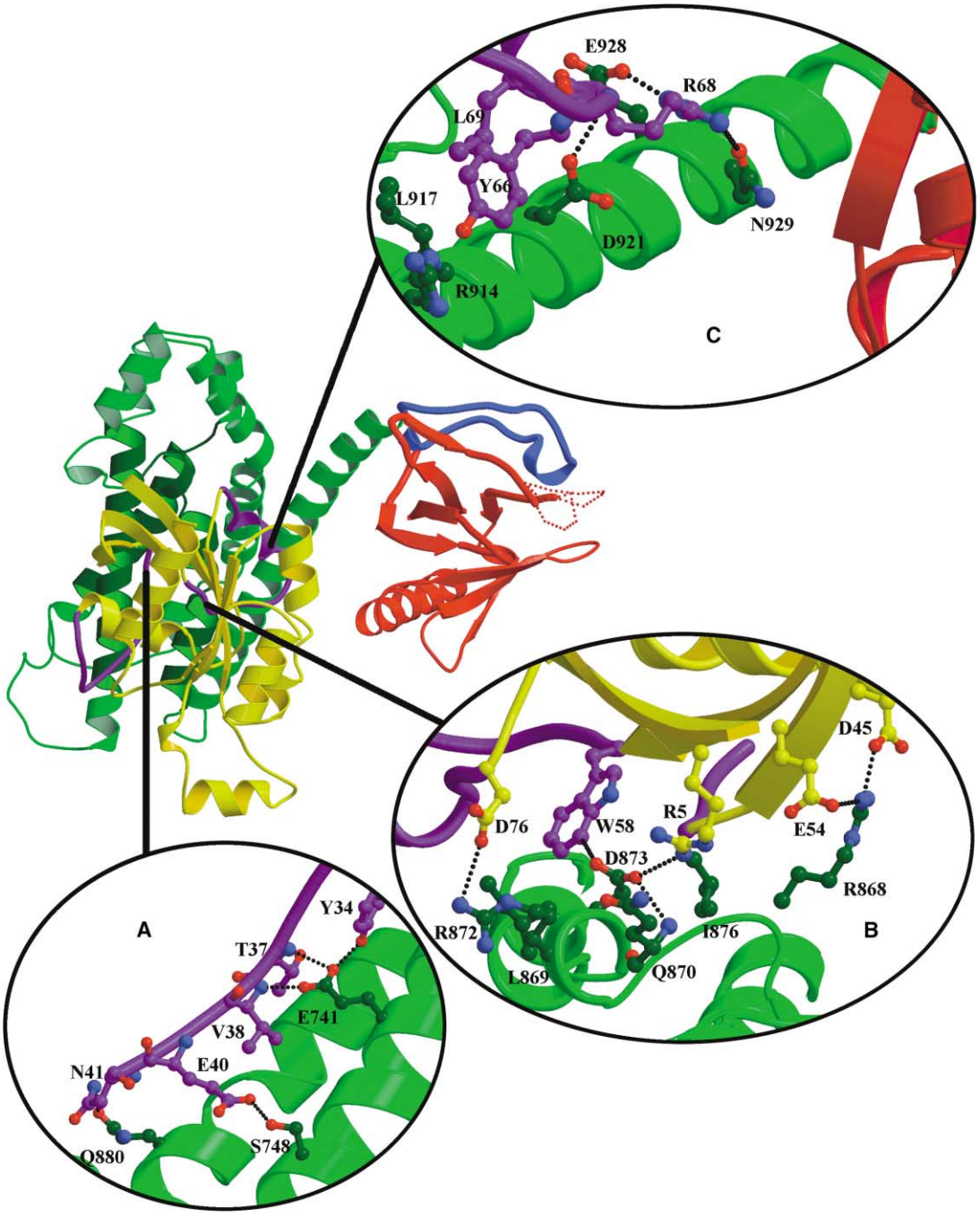

Figure 4. The Detailed View of the RhoA-DH Interface

(A) The RhoA switch I (purple) interaction with the α1a and α5b helices (green) of the DH domain; atoms are colored by type except for carbon; hydrogen bonds are dotted.

(B) A view of the central part of the RhoA-DH interface centered on $Trp58^{RhoA}$; the color scheme is as in (A), yellow indicates RhoA elements not involved in switch regions.

(C) Interactions of switch II of RhoA with α6 helix of the DH domain; the color scheme is the same with the PH domain shown in red.

and those of ITSN and PDZ-RhoGEF on the other; it is bent by ~120° at position 1240, which makes it comparable—with respect to its effective length—to that of Dbs. The other aspect of the molecular architecture is the rotation of the PH domain around the α6 helix. The kink in TIAM1 α6 makes the situation unique: the C-terminal part of the α6 rotates away from the body of the DH domain pulling behind the PH domain, so that it turns away from Rac1 and, consequently, no contacts are seen between the two (Figure 5B). In the other three structures, the PH domain is turned toward the GTPase. In Dbs the rotation of the PH domain and the shorter

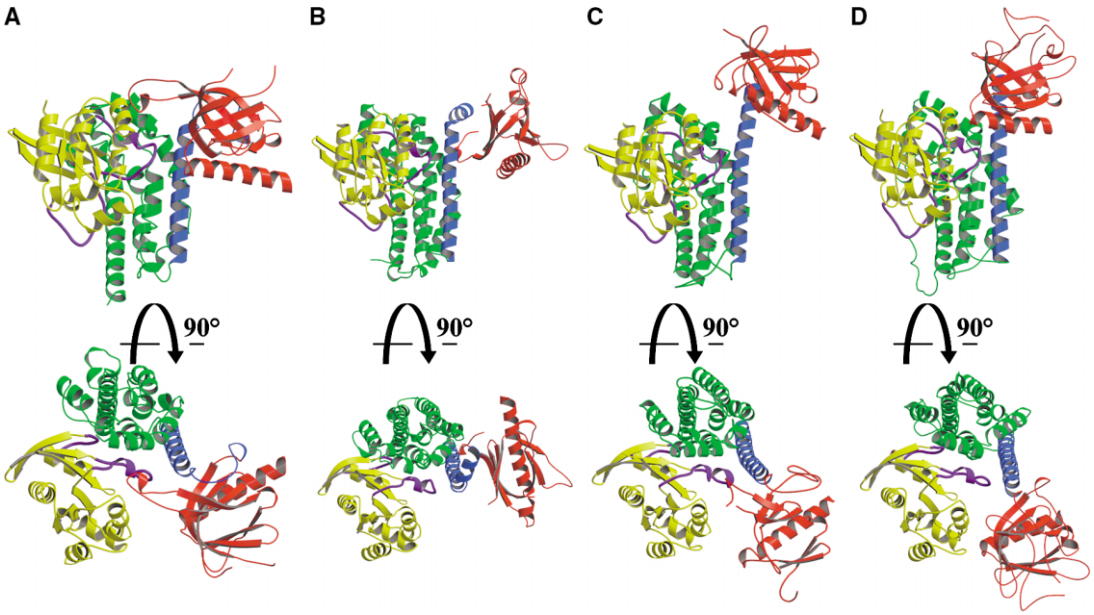

Figure 5. The Disposition of the PH Domain in Complexes of the DH/PH Fragments with Rho-GTPases

GTPases are shown in yellow, with purple switches; DH domains are in green; PH domain in red; and helix α6 of the DH domain is dark blue.
(A) Two orthogonal views of the Dbs DH/PH complex with RhoA-1LB1.PDB.
(B) TIAM1 DH/PH in complex with Rac1–1FOE.PDB.
(C) Intersectin DH/PH in complex with Cdc42-1KI1.PDB.
(D) The PDZRhoGEF DH/PH complex with RhoA reported in this paper.

length of the α6 helix bring the β3/β4 loop into contact with switch 2 of the GTPase. In the intersectin, this contact is not possible due to length of the α6 helix which extends ~16 Å further compared with Dbs (Snyder et al., 2002), despite the fact that the rotation of PH domain in ITSN (Figure 5C) is similar to Dbs. Interestingly, the structure described here resembles intersectin more than Dbs, because the length of the α6 helix is virtually identical in the two proteins (Figure 5D). However, the PH domain is rotated by ~26° further toward RhoA compared to intersectin. This is still inadequate to make the β3/β4 loop contact switch 2 of the GTPase, as seen in Dbs and the contacts that the PH domain makes with RhoA are limited to the C-terminal portion of the α3a helix and in particular Glu97 which is H-bonded to Ser1065 and Asn1068 in the C-helix of the PH domain. The associated buried surface is very limited (~260 Å^2) and accounts for only ~8% of the total buried surface in the complex. In intersectin this fraction is even lower (~4%), while in Dbs the PH/GTPase interface accounts for over 22% of the total buried surface.

Recognition of RhoA by PDZ-RhoGEF

One of the biologically most important, and medically most relevant questions is the molecular basis of the recognition of target GTPases by GEFs. While many GEFs show relative promiscuity with respect to GTPase activation, the PDZRhoGEF and its homologs show remarkable specificity toward RhoA. Furthermore, the observed enhancement of nucleotide exchange activity observed for the DH/PH fragment of PDZRhoGEF on RhoA is approximately 4-fold higher than any of the hitherto reported rates for other DH/PH tandems. The structure of the complex reveals several interesting features that allow us to hypothesize about the roots of both high selectivity and activity.

A previous elegant study (Snyder et al., 2002), based on crystallographic investigations of the complexes of intersectin and Dbs with Cdc42 and RhoA, respectively, put forward a general proposal for a mechanism of positive selection of RhoA by GEFs. According to this proposal Trp58^{RhoA} is one of the specificity determinants for those GEFs that discriminate between Cdc42, which has Phe in the analogous position, and RhoA. This bulky residue is seen in the Dbs-RhoA structure to be sequestered between Leu759^{DH} and Leu766^{DH}, equivalent in PDZRhoGEF to Leu869^{DH} and Ile876^{DH}. It has been shown that the Leu766^{DH} →Ile mutation in Dbs substantially increases its catalytic activity on RhoA, from 48-fold to 267-fold (Cheng et al., 2002), with little impact on Cdc42 (Cheng et al., 2002). This mutation also confers 57-fold rate enhancement on Dbs against Rac (Cheng et al., 2002). In PDZRhoGEF, the equivalent position is occupied by a RhoA-preferred Ile.

It was also noted (Snyder et al., 2002) that both Asp45 and Glu54 are unique to RhoA, and are replaced by small and neutral residues in both Rac and Cdc42. All GEFs active on RhoA have Lys or Arg in a position equivalent to Lys758^{DH} of Dbs, which forms a double salt-bridge with Asp45 and Glu54 (Snyder et al., 2002). Indeed, the PDZRhoGEF has an Arg in this position (Arg868^{DH}), as do its homologs LARG and p115. Another suggested determinant was Arg5^{RhoA}, which was thought to make a favorable interaction with a Gln residue in RhoA specific GEFs. Our structure shows that Arg5^{RhoA} is indeed involved, but in a dramatically different way,

Table 2. Crystallographic Data

	SeMet Peak	SeMet Inflection	SeMet Remote	Native
Data collection				
Wavelength (Å)	0.9790	0.97919	0.97178	1.00
Resolution (Å)	2.6(2.69–2.6)[a]	2.6(2.69–2.6)	2.6(2.69–2.6)	2.5(2.59–2.5)
No. of total reflections	206,030	174,079	179,000	213,477
No. of unique reflections	98,601	95,011	96,264	58,062
Completeness (%)	97.7 (87.5)	94.3(71.5)	94.0 (63.5)	97.4 (83.1)
R_{merge} (%)[b]	4.6 (45.3)	4.2 (35.5)	4.2 (38.0)	5.5 (28.1)
$I/\sigma(I)$	17.6 (1.7)	16.5 (2.0)	16.1 (1.8)	21.5 (4.0)
Phasing statistics				
Phasing power[c], iso/ano	0.7/1.7	1.3/1.0	–/1.1	
Refinement statistics				
Model Composition			1069 residues + 90 waters	
Resolution limits (Å)			25–2.5	
Reflections in working/test sets			54,415/2,899	
Reflections in final refinement			57,314	
$R^{\S}/R_{free}$ (%)			22.4/28.1	
Final R[d] (%) using all data			23.5	
Bond(Å)/angle(°) rms			0.011/1.268	
Ramachadran plot				
Most favored regions			90.2%	
Additional allowed regions			8.8%	

[a] The numbers in parentheses describe the relevant value for the last resolution shell.
[b] $R_{merge} = \Sigma|I_i - \langle I \rangle|/\Sigma I$ where I_i is the intensity of the i-th observation and $\langle I \rangle$ is the mean intensity of the reflections.
[c] Phasing power = rms ($|F_h|/E$), where $|F_h|$ is the heavy atom structure factor amplitude and E is residual lack of closure error.
[d] $R = \Sigma||F_{obs}| - |F_{calc}||/\Sigma|F_{obs}|$, crystallographic R factor, and $R_{free} = \Sigma||F_{obs}| - |F_{calc}||/\Sigma|F_{obs}|$ where all reflections belong to a test set of randomly selected data.

i.e., by swinging inside the interface to make a salt-bridge with a buried $Asp873^{DH}$. A perusal of known sequences of GEFs indicates that this residue may indeed constitute an important determinant. It is found in this position in all three members of the PDZRhoGEF family, and also in Lsc, Trio/C, Vav, and Vav2, all of which are active on RhoA. Further, Lbc and Lfc, both of which are known to act on RhoA (Glaven et al., 1996) have a Glu in this position, suggesting a similar function.

In addition to these predicted interactions, our structure reveals additional features that may substantially enhance the selectivity and activity of PDZRhoGEF and its homologs. Of particular interest are two salt bridges, $Arg872^{DH}$ with $Asp76^{RhoA}$ and $Arg867^{DH}$ with $Glu40^{RhoA}$. Position 872 is occupied in the PDZRhoGEF family GEFs by Arg or Lys, and a favorable interaction is possible uniquely with RhoA, because the position equivalent to the charged Asp76 is occupied by a neutral Gln in both Cdc42 and Rac. $Arg867^{DH}$ is conserved among the PDZRhoGEF family members, and the position is often occupied by positively charged residues in other GEFs acting on RhoA, such as Lbc or Lfc. Altogether, the PDZRhoGEF–RhoA interface contains a number of highly selective interactions, involving a number of salt bridges, exploiting the unique electrostatic potential surface of RhoA.

Conclusion

In this paper, we present evidence that PDZRhoGEF is a likely candidate to serve as a molecular coupling between G protein-coupled receptors and RhoA in smooth muscle, with a potentially critical role in Ca^{2+} sensitization. It was recently shown, that in the HEK 293T and PC-3 prostate cancer cells, the thrombin receptor activates RhoA via LARG, while the LPA stimulation of RhoA is due to PDZRhoGEF (Wang et al., 2004). Thus, the RGSL-containing family of nucleotide exchange factors emerges as a physiologically important and ubiquitous class of signaling molecules. The 2.5 Å resolution crystal structure of the complex of the DH/PH fragment with RhoA, reported here, reveals an extensive and specific interface between the DH domain and the GTPase, fully rationalizing the observed specificity and selectivity of PDZRhoGEF and its homologs. In addition to the expected interactions involving Trp58 of RhoA and the residues in the α5 helix of the DH domain, we identified several other interactions unique for RhoA, notably those involving Arg5, Asp76, and Asp40. Further mutational studies will establish the individual contributions of these interactions to the overall selectivity of PDZRhoGEF and other members in this family. The PH domain makes contact with RhoA, but the resulting interface is small, and it is not immediately obvious if the PH domain participates directly in catalysis, as seems to be suggested by the in vitro nucleotide exchange assays. The structure suggests, however, that the PH domain might be involved indirectly, by providing stabilization to the C-terminal part of the α6 helix of the DH domain. Further experiments, under way in our laboratories, will resolve this issue.

While this paper was being reviewed, a study of a related complex involving the DH/PH fragment of LARG was published online ahead of print (Kristelly et al., 2004). In spite of significantly lower resolution of data than those reported here (i.e., 3.2 Å versus 2.5 Å), the authors observe a mutual disposition of the DH/PH and RhoA molecules that appears to be consistent with our

results. Detailed comparison will be possible upon the release of the coordinates.

Experimental Procedures

Expression and Purification

The DH/PH fragment (residues 712–1081) and DH domain (residues 729–939) of human PDZ-RhoGEF were expressed as fusion proteins with GST in BL21(DE3)-RIL *E. coli* strain (Stratagene). Both fusion proteins were purified as described previously (Oleksy et al., 2004), except for using an anion exchanger HiTrap Q Sepharose (Amersham Pharmacia Biotech) instead of Superdex-75 size exclusion column (Amersham Pharmacia Biotech). The purified DH/PH and DH proteins were concentrated in 50 mM Tris-HCl, [pH 7.5], 20 mM NaCl, and 1 mM DTT. Human full-length RhoA (residues 1–193), truncated RhoA (residues 1–181), full-length Cdc42 (1–191 aa), and full-length Rac1 (residues 1–192) were expressed in pETUni vector (Sheffield et al., 1999) in fusion with a His_6-tag also in BL21(DE3) RIL. The GTPases were purified by Ni-NTA-agarose affinity chromatography in 50 mM Tris-HCl, 400 mM NaCl, 1 mM $MgCl_2$, 5 mM imidazole, [pH 8.0], and eluted with 150 mM imidazole buffer. Final purification was carried out using gel filtration. Before fluorescence exchange assays, bacterially expressed RhoA, Cdc42, and Rac1 were incubated with excess GDP (ICN Biomedicals, Inc.) in the presence of EDTA. After 1 hr, excess of $MgCl_2$ was added and the unbound nucleotide was removed using a HiPrep desalting column (Amersham Pharmacia Biotech).

The SeMet labeled DH/PH tandem was expressed using the $pHis_6MBP$ vector (gift from Dr. D. Waugh, NCI) and the Met auxotroph DL41 *E. coli* strain. The cultures were grown in the LeMaster media at 37°C. Protein expression was induced at a high OD_{600} of ~3.5 with 1 mM IPTG. The cultures were incubated at room temperature for 24 hr. The cells were harvested by centrifugation. The pellet was resuspended in lysis buffer (50 mM Tris-HCl, [pH 7.5], 300 mM NaCl, 5 mM Met, and 10 mM imidazole) and disrupted. The supernatant was incubated at 4°C with Ni-NTA (Qiagen) resin for 1 hr. After washing the resin with 4 liter of lysis buffer, the protein was eluted in 1 ml fractions with elution buffer (lysis buffer containing 150 mM imidazole). Fractions containing the HisMBP-DH/PH fusion protein were incubated overnight with the rTEV proteinase (Kapust et al., 2001) at 10°C. After removal of imidazole using a desalting column, the SeMet labeled DH/PH was separated from cleaved HisMBP using Ni-NTA resin as described above. The concentrated protein was further purified using size-exclusion chromatography column (Superdex 200 16/60, Amersham Pharmacia Biotech) and mixed with excess amount of F25N mutant of truncated RhoA. The sample was dialyzed against 20 mM Tris-HCl, 150 mM NaCl, 1 mM DTT, and 5 mM EDTA [pH 7.1] overnight at 4°C in order to remove Mg^{+2} and the nucleotide. The SeMet DH/PH–RhoA complex was purified from excess of RhoA using Superdex 200 size-exclusion column equilibrated with 20 mM Tris-HCl, [pH 7.2], 150 mM NaCl, and 1 mM TCEP.

Western Blot Analysis for PDZ-RhoGEF

Supernatants from whole tissue homogenate were solubilized in 1× Laemmli sample buffer and clarified (800 × *g*, 10 min) before SDS-PAGE. Homogenates were run on 10% SDS-PAGE and were transferred to PVDF (polyvinylidene difluoride) membranes. Membranes were blocked with 5% nonfat dry milk in phosphate-buffered saline containing 0.05% Tween-20 (PBS-T) for 1 hr at room temperature. Membranes were incubated overnight at 4°C (1:1000) in a polyclonal primary antibody for PDZ-RhoGEF prepared in rabbit, a gift from Dr. Silvio Gutkind, followed by washing in PBS-T and incubation with horseradish peroxidase-conjugated secondary antibody to rabbit for 1 hr at room temperature and developed with enhanced chemiluminescence (ECL, Amersham Pharmacia Biotech). Membranes were stripped and reblotted with a smooth muscle anti-α-actin antibody to normalize for protein load.

Guanine Nucleotide Exchange Assay

Fluorescence spectroscopic analysis using the N-methylanthraniloyl-GTP (mant-GTP) was performed with a Jasco FP-750 spectrofluorimeter. Mant-GTP was synthesized according to the published procedure (Hiratsuka, 1983). The exchange reaction was carried out at 21°C, in a quartz cuvette containing 1 μM GDP-preloaded RhoA, Cdc42, or Rac1, and 500 nM mant-GTP in 20 mM Tris-HCl, [pH 7.5], 50 mM NaCl, 5 mM $MgCl_2$, 1 mM DTT, and 5% glycerol, continuously stirred at 450 rpm. After ~300 s equilibration time, the DH domain or DH/PH tandem was added at 100 nM and the mant-GTP fluorescence increase was monitored (λ_{ex} = 356 nm, λ_{em} = 445 nm) as a result of its incorporation to the GTPase. The control experiment reflects intrinsic exchange activity of a given GTPase, measured after equivalent equilibration time. Each exchange experiment was carried out three times independently. The initial rates of guanine nucleotide exchange were determined by linear regression analysis of approximately the first 50 s after DH stimulation and 12 s after DH/PH stimulation. Although the rates for RhoA were previously reported by us (Oleksy et al., 2004), they were repeated in this study to ensure that the experimental conditions were identical to those for Rac and Cdc42. The discrepancies between the two sets of data are due to the higher level of purity of the DH-PH fragment in this study.

Tissue Preparation and Isometric Tension Measurements

Male white New Zealand Rabbits (2–3 kg) were anesthetized by overdose with halothane. Pulmonary artery was removed, placed into warm HEPES-buffered Krebs solution, [pH 7.3]. The connective tissue and adventitia were carefully removed and thin strips (100–200 μM wide and 1–2 mm long) were dissected and stretched by 10% of resting length. Isometric tension was measured with a force transducer (AE801; Akers, Horten, Norway) on a "bubble" plate (Kitazawa et al., 1989). Strips were incubated in a Ca^{2+}-free normal relaxing solution containing 1 mM EGTA (G1) and permeabilized with β-escin (75μM) for 30 min at 22°C. To deplete the sacroplasmic reticulum of calcium, all permeabilized strips were treated with A23187 (10 μM; Calbiochem, La Jolla, CA) for 10 min in relaxing solution (Kitazawa et al., 1989; Kobayashi et al., 1991). Permeabilized strips were incubated with a solution containing 10 mM EGTA and sufficient Ca for a final free pCa 6.7. Following incubation, the DH/PH domain of PDZ-RhoGEF (50 μM) or filtrate was added to the pCa 6.7 solution and force was observed. The pretreatment of the strips with A23187, buffering with EGTA as well as the lack of effect of the filtrate, assert that the changes in force were not due to changes in Ca^{2+} concentration.

Crystallization and Data Collection

The SeMet DH/PH–RhoA crystals were grown by vapor diffusion in hanging drops at room temperature by adding 1.5 μl of well solution (200 mM tripotassium citrate [pH 7.9], 21% PEG 3350, 0.5 mM EDTA, and 2 mM TCEP) to 1.5μl of protein complex at 12 mg/mL concentration. The crystals grew to average dimensions of 0.2 mm × 0.2 mm × 0.2 mm within 2 weeks. The best cryosolution proved to be 32% PEG 3350, 16% glycerol, and 500 mM KI, with KI greatly improving the diffraction quality. For data collection, the largest crystal 0.4 × 0.2 × 0.24 mm was transferred to the cryosolution and frozen. The crystals belong to space group, $P2_1$, a = 87.9 Å, b = 118.8 Å, c = 88.7 Å, and β = 113.5°. A MAD data set was collected on beamline X9B at the NSLS (Brookhaven National Laboratory) at Se absorption peak (λ_1 = 0.9790 Å), edge (λ_2 = 0.97919 Å) and a remote wavelength (λ_3 = 0.97178 Å). Data were integrated and scaled using HKL2000 (Otwinowski and Minor, 1997).

Phasing, Model Building, and Refinement

Fourteen out of sixteen Se atoms were located using anomalous differences by SHELXD (Schneider and Sheldrick, 2002). MAD phases were calculated and refined in SHARP (Fortelle and Bricogne, 1997) using remote wavelength as the reference dataset. Fourier maps were used to locate the remaining two selenium atoms. Solvent flattening was performed using Solomon and DM as implemented in SHARP. These phases were sufficient to trace most of RhoA molecules and DH domains. Only partial models of the PH domains were traced at this stage since the electron density for these regions remained poorly defined. Multidomain averaging made it possible to build the remainder of the structure. The NCS averaging was performed using RAVE (Kleywegt and Jones, 1994). Program O (Jones et al., 1991) was used for model building and

Refmac5 (Murshudov et al., 1997) for refinement. NCS restrains were applied throughout the refinement. The final refinement was carried out using native data at 2.5 Å resolution. At the stage when R_{cryst} was 22.4% and R_{free} was 28.1%, the model was refined against all reflections. The final model contains 9252 atoms (8661 protein and 591 solvent atoms). The model has 90.3% of all residues in the core region of the Ramachandran plot with no residues in the disallowed regions. The mean temperature (B) factor for all atoms is 65.8 $Å^2$ (Table 2).

Acknowledgments

We gratefully acknowledge Holly Barton, Natalya Olekhnovich (University of Virginia), and Agnieszka Gajewska-Naryniecka (University of Wrocław) for excellent technical assistance. We also thank Filip Jeleń (University of Wrocław) for providing mant-GTP and Rho-GTPases; Dr. Silvio Gutkind (NIH) for the PDZRhoGEF antibody; Dr. David Waugh (NCI) for the $pHis_6MBP$ vector; and Dr. David Cooper (UVA) for help with computing and figure preparation. This work was supported by an NIH Grant PO1 HL48807 to A.V.S. The Z.S.D. and J.O. groups are also supported by a NATO Collaborative Link Grant. J.O. is a Howard Hughes International Scholar.

Received: July 18, 2004
Revised: September 3, 2004
Accepted: September 13, 2004
Published online: September 23, 2004

References

Aghazadeh, B., Zhu, K., Kubiseski, T.J., Liu, G.A., Pawson, T., Zheng, Y., and Rosen, M.K. (1998). Structure and mutagenesis of the Dbl homology domain. Nat. Struct. Biol. *5*, 1098–1107.

Chan, A.W., Hutchinson, E.G., Harris, D., and Thornton, J.M. (1993). Identification, classification, and analysis of beta-bulges in proteins. Protein Sci. *2*, 1574–1590.

Chen, Z., Wells, C.D., Sternweis, P.C., and Sprang, S.R. (2001). Structure of the rgRGS domain of p115RhoGEF. Nat. Struct. Biol. *8*, 805–809.

Cheng, L., Rossman, K.L., Mahon, G.M., Worthylake, D.K., Korus, M., Sondek, J., and Whitehead, I.P. (2002). RhoGEF specificity mutants implicate RhoA as a target for Dbs transforming activity. Mol. Cell. Biol. *22*, 6895–6905.

Derewenda, Z.S., Lee, L., and Derewenda, U. (1995). The occurrence of C-H.O hydrogen bonds in proteins. J. Mol. Biol. *252*, 248–262.

Dutt, P., Nguyen, N., and Toksoz, D. (2004). Role of Lbc RhoGEF in $G\alpha_{12/13}$-induced signals to Rho GTPase. Cell. Signal. *16*, 201–209.

Fortelle, E.D.l., and Bricogne, G. (1997). Maximum-likelihood heavy atom parameter refinement for multiple isomorphous replacement and multiwavelength anomalous diffraction methods. Methods Enzymol. *276*, 472–494.

Fukuhara, S., Murga, C., Zohar, M., Igishi, T., and Gutkind, J.S. (1999). A novel PDZ domain containing guanine nucleotide exchange factor links heterotrimeric G proteins to Rho. J. Biol. Chem. *274*, 5868–5879.

Fukuhara, S., Chikumi, H., and Gutkind, J.S. (2000). Leukemia-associated Rho guanine nucleotide exchange factor (LARG) links heterotrimeric G proteins of the G(12) family to Rho. FEBS Lett. *485*, 183–188.

Glaven, J.A., Whitehead, I.P., Nomanbhoy, T., Kay, R., and Cerione, R.A. (1996). Lfc and Lsc oncoproteins represent two new guanine nucleotide exchange factors for the Rho GTP-binding protein. J. Biol. Chem. *271*, 27374–27381.

Gong, M.C., Iizuka, K., Nixon, G., Browne, J.P., Hall, A., Eccleston, J.F., Sugai, M., Kobayashi, S., Somlyo, A.V., and Somlyo, A.P. (1996). Role of guanine nucleotide-binding proteins—Ras-family or trimeric proteins or both—in Ca^{2+} sensitization of smooth muscle. Proc. Natl. Acad. Sci. USA *93*, 1340–1345.

Hart, M.J., Jiang, X., Kozasa, T., Roscoe, W., Singer, W.D., Gilman, A.G., Sternweis, P.C., and Bollag, G. (1998). Direct stimulation of the guanine nucleotide exchange activity of p115 RhoGEF by $G\alpha13$. Science *280*, 2112–2114.

Himpens, B., Kitazawa, T., and Somlyo, A.P. (1990). Agonist-dependent modulation of Ca^{2+} sensitivity in rabbit pulmonary artery smooth muscle. Pflugers Arch. *417*, 21–28.

Jackson, M., Song, W., Liu, M.Y., Jin, L., Dykes-Hoberg, M., Lin, C.I., Bowers, W.J., Federoff, H.J., Sternweis, P.C., and Rothstein, J.D. (2001). Modulation of the neuronal glutamate transporter EAAT4 by two interacting proteins. Nature *410*, 89–93.

Jiang, L., and Lai, L. (2002). CH.O hydrogen bonds at protein-protein interfaces. J. Biol. Chem. *277*, 37732–37740.

Jones, T.A., Zou, J.Y., Cowan, S.W., and Kjeldgaard, M. (1991). Improved methods for binding protein models in electron density maps and the location of errors in these models. Acta Crystallogr. *A47*, 110–119.

Kapust, R.B., Tozser, J., Fox, J.D., Anderson, D.E., Cherry, S., Copeland, T.D., and Waugh, D.S. (2001). Tobacco etch virus protease: mechanism of autolysis and rational design of stable mutants with wild-type catalytic proficiency. Protein Eng. *14*, 993–1000.

Karnoub, A.E., Worthylake, D.K., Rossman, K.L., Pruitt, W.M., Campbell, S.L., Sondek, J., and Der, C.J. (2001). Molecular basis for Rac1 recognition by guanine nucleotide exchange factors. Nat. Struct. Biol. *8*, 1037–1041.

Kitazawa, T., Kobayashi, S., Horiuti, K., Somlyo, A.V., and Somlyo, A.P. (1989). Receptor-coupled, permeabilized smooth muscle. Role of the phosphatidylinositol cascade, G-proteins, and modulation of the contractile response to Ca^{2+}. J. Biol. Chem. *264*, 5339–5342.

Kleywegt, G.J., and Jones, T.A. (1994). Halloween masks and bones. Proceedings of the CCP4 study weekend. January *6-7*, 59–66.

Kobayashi, S., Gong, M.C., Somlyo, A.V., and Somlyo, A.P. (1991). Ca^{2+} channel blockers distinguish between G protein-coupled pharmacomechanical Ca^{2+} release and Ca^{2+} sensitization. Am. J. Physiol. *260*, C364–C370.

Kozasa, T., Jiang, X., Hart, M.J., Sternweis, P.M., Singer, W.D., Gilman, A.G., Bollag, G., and Sternweis, P.C. (1998). p115 RhoGef, a GTPase activating protein for $G\alpha_{12}$ and $G\alpha_{13}$. Science *280*, 2109–2111.

Kristelly, R., Gao, G., and Tesmer, J.J.G. (2004). Structural determinants of RhoA binding and nucleotide exchange in leukemia-associated RhoGEF. J. Biol. Chem., in press. Published online August 25, 2004. 10.1074/jbc.M406056200.

Lemmon, M.A., Ferguson, K.M., and Abrams, C.S. (2002). Pleckstrin homology domains and the cytoskeleton. FEBS Lett. *513*, 71–76.

Liu, X., Wang, H., Eberstadt, M., Schnuchel, A., Olejniczak, E.T., Meadows, R.P., Schkeryantz, J.M., Janowick, D.A., Harlan, J.E., Harris, E.A., et al. (1998). NMR structure and mutagenesis of the N-terminal Dbl homology domain of the nucleotide exchange factor Trio. Cell *95*, 269–277.

Longenecker, K.L., Lewis, M.E., Chikumi, H., Gutkind, J.S., and Derewenda, Z.S. (2001). Structure of the RGS-like domain from PDZ-RhoGEF: linking heterotrimeric G protein-coupled signaling to Rho GTPases. Structure *9*, 559–569.

Macias, M.J., Musacchio, A., Ponstingl, H., Nilges, M., Saraste, M., and Oschkinat, H. (1994). Structure of the pleckstrin homology domain from β-spectrin. Nature *369*, 675–677.

Murshudov, G.N., Vagin, A.A., and Dodson, E.J. (1997). Refinement of macromolecular structures by the maximum-likelihood method. Acta Crystallogr. *D53*, 240–255.

Oleksy, A., Barton, H., Devedjiev, Y., Purdy, M., Derewenda, U., Otlewski, J., and Derewenda, Z.S. (2004). Preliminary crystallographic analysis of the complex of the human GTPase RhoA with the DH/PH tandem of PDZ-RhoGEF. Acta Crystallogr. *D60*, 740–742.

Otwinowski, Z., and Minor, W. (1997). Processing of X-ray diffraction data collected in oscillation mode. Methods Enzymol. *A276*, 307–326.

Petrella, R.J., and Karplus, M. (2004). The role of carbon-donor hydrogen bonds in stabilizing tryptophan conformations. Proteins *54*, 716–726.

Pierce, A.C., Sandretto, K.L., and Bemis, G.W. (2002). Kinase inhibitors and the case for CH.O hydrogen bonds in protein-ligand binding. Proteins *49*, 567–576.

Pruitt, W.M., Karnoub, A.E., Rakauskas, A.C., Guipponi, M., Antonarakis, S.E., Kurakin, A., Kay, B.K., Sondek, J., Siderovski, D.P., and Der, C.J. (2003). Role of the pleckstrin homology domain in intersectin-L Dbl homology domain activation of Cdc42 and signaling. Biochim. Biophys. Acta *1640*, 61–68.

Rebecchi, M.J., and Scarlata, S. (1998). Pleckstrin homology domains: a common fold with diverse functions. Annu. Rev. Biophys. Biomol. Struct. *27*, 503–528.

Rossman, K.L., and Campbell, S.L. (2000). Bacterial expressed DH and DH/PH domains. Methods Enzymol. *325*, 25–38.

Rossman, K.L., Worthylake, D.K., Snyder, J.T., Siderovski, D.P., Campbell, S.L., and Sondek, J. (2002). A crystallographic view of interactions between Dbs and Cdc42: PH domain-assisted guanine nucleotide exchange. EMBO J. *21*, 1315–1326.

Rumenapp, U., Blomquist, A., Schworer, G., Schablowski, H., Psoma, A., and Jakobs, K.H. (1999). Rho-specific binding and guanine nucleotide exchange catalysis by KIAA0380, a dbl family member. FEBS Lett. *459*, 313–318.

Schmidt, A., and Hall, A. (2002). Guanine nucleotide exchange factors for Rho GTPases: turning on the switch. Genes Dev. *16*, 1587–1609.

Schneider, T.R., and Sheldrick, G.M. (2002). Substructure solution with SHELXD. Acta Crystallogr. *D58*, 1772–1779.

Sheffield, P., Garrard, S., and Derewenda, Z. (1999). Overcoming expression and purification problems of RhoGDI using a family of "Parallel" expression vectors. Protein Expr. Purif. *15*, 34–39.

Snyder, J.T., Worthylake, D.K., Rossman, K.L., Betts, L., Pruitt, W.M., Siderovski, D.P., Der, C.J., and Sondek, J. (2002). Structural basis for the selective activation of Rho GTPases by Dbl exchange factors. Nat. Struct. Biol. *9*, 468–475.

Soisson, S.M., Nimnual, A.S., Uy, M., Bar-Sagi, D., and Kuriyan, J. (1998). Crystal structure of the Dbl and pleckstrin homology domains from the human Son of sevenless protein. Cell *95*, 259–268.

Somlyo, A.P., and Somlyo, A.V. (2003). Ca2+ sensitivity of smooth muscle and nonmuscle myosin II: modulated by G proteins, kinases, and myosin phosphatase. Physiol. Rev. *83*, 1325–1358.

Suzuki, N., Nakamura, S., Mano, H., and Kozasa, T. (2003). $G\alpha_{12}$ activates Rho GTPase through tyrosine-phosphorylated leukemia-associated RhoGEF. Proc. Natl. Acad. Sci. USA *100*, 733–738.

Wang, Q., Liu, M., Kozasa, T., Rothstein, J.D., Sternweis, P.C., and Neubig, R.R. (2004). Thrombin and lysophosphatidic acid receptors utilize distinct rhoGEFs in prostate cancer cells. J. Biol. Chem. *279*, 28831–28834.

Whitehead, I.P., Campbell, S., Rossman, K.L., and Der, C.J. (1997). Dbl family proteins. Biochim. Biophys. Acta *1332*, F1–23.

Worthylake, D.K., Rossman, K.L., and Sondek, J. (2000). Crystal structure of Rac1 in complex with the guanine nucleotide exchange region of Tiam1. Nature *408*, 682–688.

Worthylake, D.K., Rossman, K.L., and Sondek, J. (2004). Crystal structure of the DH/PH fragment of Dbs without bound GTPase. Structure *12*, 1079–1086.

Accession Numbers

The atomic coordinates were deposited in the Protein Data Bank, Research Collaboratory for Structural Bioinformatics, Rutgers University, New Brunswick, New Jersey under the accession code 1xcg.pdb.